The Quadrupole Resonator: a Tool to Study RF Superconductors

Raphael Kleindienst Jens Knobloch Oliver Kugeler Sebastian Keckert Andrew Burrill

SRF 2015
Whistler
16.09.2015

Helmholtz Zentrum Berlin

Introduction

Many features in QvsE curves

- Complex theory required to describe RF properties of superconductors
- Systematic test of theory difficult

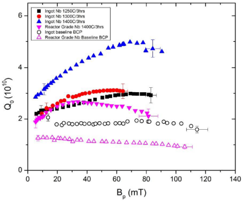

Doped/ Undoped bulk niobium [1]

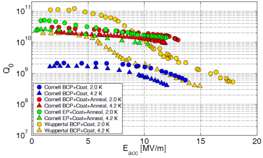

Nb_3Sn [2]

[1] P. Dhakal et al., "Enhancement in Quality Factor of SRF Niobium Cavities by Material Diffusion".

[2] Posen and Liepe, "Nb3Sn - Present Status and Potential as an alternative SRF Material".

Many features in QvsE curves

- Complex theory required to describe RF properties of superconductors
- Systematic test of theory difficult

How does ideal experiment look like?

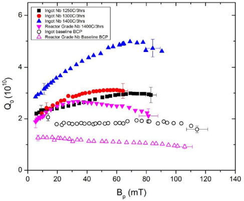

Doped/ Undoped bulk niobium [1]

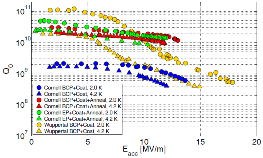

Nb_3Sn [2]

[1] P. Dhakal et al., "Enhancement in Quality Factor of SRF Niobium Cavities by Material Diffusion".

[2] Posen and Liepe, "Nb3Sn - Present Status and Potential as an alternative SRF Material".

Introduction

Many features in QvsE curves

- Complex theory required to describe RF properties of superconductors
- Systematic test of theory difficult

How does ideal experiment look like?

- Small and flat samples, easy to change
- Measure RF losses in large parameter space:
  - Wide temperature range, high RF field
  - Multiple frequencies (not too high)
  - Control over ambient magnetic field and cooling conditions
- Penetration depth, critical field, RRR, heat conductivity

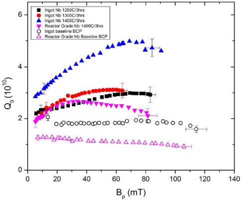

Doped/ Undoped bulk niobium [1]

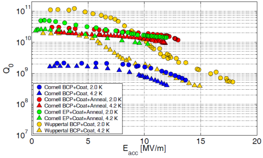

Nb_3Sn [2]

[1] P. Dhakal et al., "Enhancement in Quality Factor of SRF Niobium Cavities by Material Diffusion".
[2] Posen and Liepe, "Nb3Sn - Present Status and Potential as an alternative SRF Material".

Quadrupole Resonator

Niobium cavity for sample testing pioneered at CERN in late 1990's. [1]
Strong focusing of magnetic fields on sample surface allow measurement of RF losses

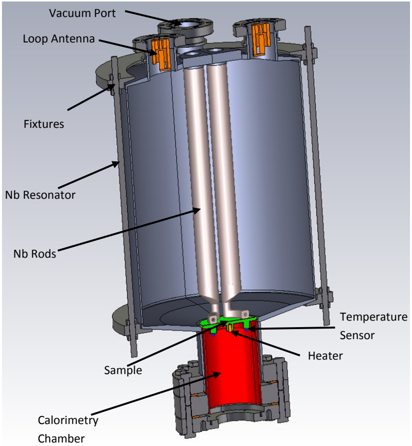

Advantages

- Sample thermally decoupled from resonator and helium bath
- Calorimetric measurement → high resolution
- Measurements at 400, 800 and 1200 MHz
- Penetration depth and critical field measurements possible

Disadvantages

- Large sample (75mm), difficult to change
- Inhomogenous field on sample surface, $\langle R_s \rangle$ measurement

[1] Haebel, Brigant, and Mahner, "The Quadrupole Resonator, Design Considerations and Layout of a new Instrument for the RF Characterization of Superconducting Surface".

RF optimization

CERN geometry adapted to include 1300 MHz mode used as baseline,
Aim of optimization:

- Increase measurement range:
  - $\rightarrow$ Decrease peak field ratios $\mathrm{E_{pk}}/\mathrm{B_{smpl}}$ and $\mathrm{B_{pk}}/\mathrm{B_{smpl}}$
- Improve measurement resolution:
  - $\rightarrow$ Increase focussing of magnetic fields on to sample: $c = \frac{\int_{\mathrm{Smpl}} |H|^2 dA}{U}$

	Baseline	Optimized
c	$5.15 \cdot 10^7\ \mathrm{A^2/J}$	$11.2 \cdot 10^7\ \mathrm{A^2/J}$
$\mathrm{E_{pk}}/\mathrm{B_{smpl}}$	$0.21\,\mathrm{(MV/m)/mT}$	$0.13\,\mathrm{(MV/m)/mT}$
$\mathrm{B_{pk}}/\mathrm{B_{smpl}}$	1.23	1.12
1^{st} Mechanical mode	69 Hz	120 Hz

Comparison figures of merit [1]

[1] Kleindienst, Knobloch, and Kugeler, "Development of an Optimized Quadrupole Resonator at HZB".

Production

HZB QPR built by Niowave

- RRR300 fine-grain Niobium
- Mechanical design simplified, wall thickness 2 mm

Surface finishing at JLab:

- 150 $\mu\mathrm{m}$ BCP,
- 600 $^{\circ}\mathrm{C}$ bake for 12 hours
- High Pressure Rinse, 55 bar jet shooting upwards through the rods from the below the loops
- 20 $\mu\mathrm{m}$ light - BCP
- 120 $^{\circ}\mathrm{C}$ bake for 48 h

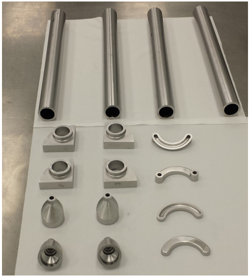

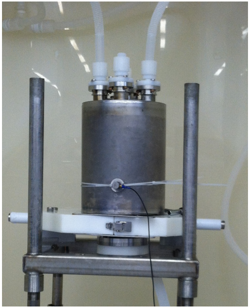

QPR at HZB

Characterization Niobium Sample

Large grain RRR 300 Niobium sample (undoped) with 120° bake.
Surface resistance measured against field at 416 MHz .

- RF losses measured at various temperature with fields up to $> 100\,\mathrm{mT}$
- Decreasing surface resistance at medium fields for low temperatures
- Plotting against temperature yields consistent residual resistance around $7.5\,\mathrm{n\Omega}$

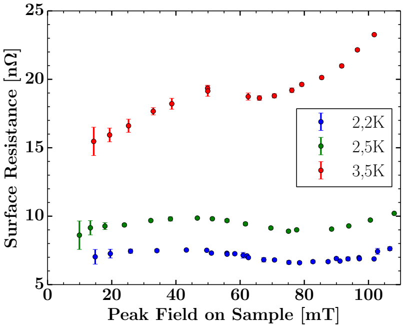

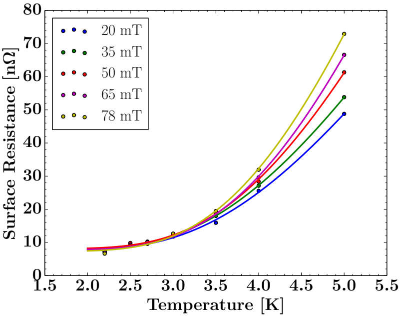

Potential error source

Temperature Gradient

- Heater and RF field generate different temperature gradient
- Changing RF field changes temperature gradient
- Different temperature gradient leads to different losses

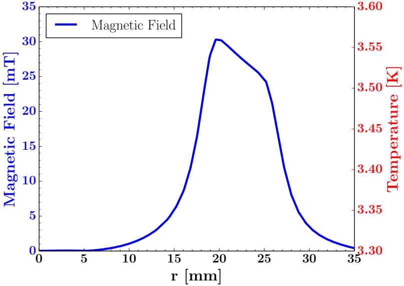

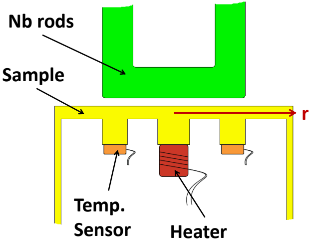

Temperature Gradient

- Heater and RF field generate different temperature gradient
- Changing RF field changes temperature gradient
- Different temperature gradient leads to different losses

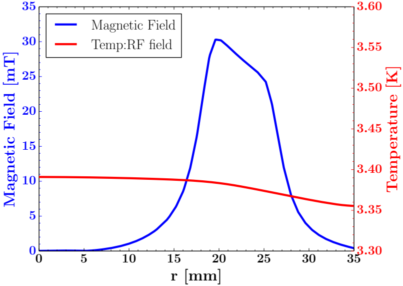

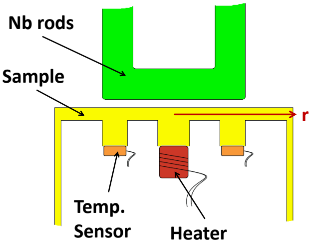

Potential error source

Temperature Gradient

- Heater and RF field generate different temperature gradient
- Changing RF field changes temperature gradient
- Different temperature gradient leads to different losses

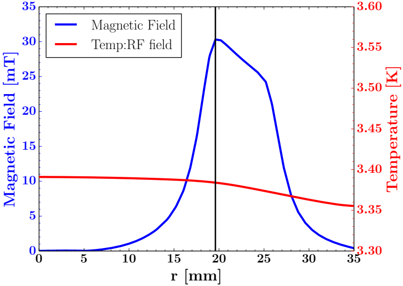

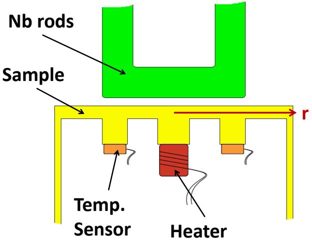

Temperature Gradient

- Heater and RF field generate different temperature gradient
- Changing RF field changes temperature gradient
- Different temperature gradient leads to different losses

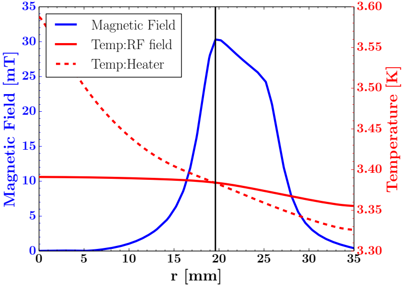

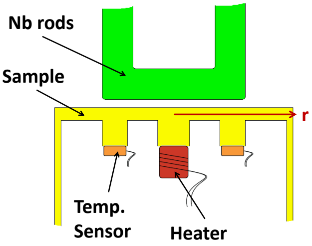

Potential error source

Temperature Gradient

- Heater and RF field generate different temperature gradient
- Changing RF field changes temperature gradient
- Different temperature gradient leads to different losses

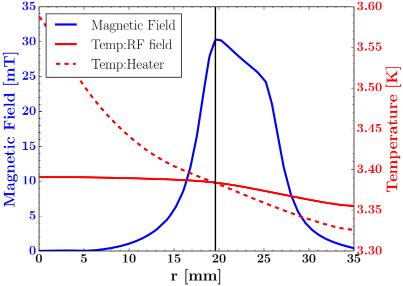

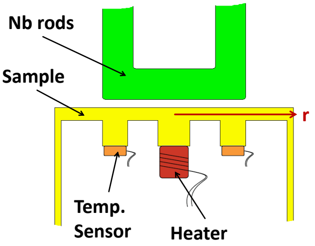

Ring shaped heater (no temperature gradient) required

Trapped Flux Measurement

Copper solenoid and magnetometer mounted within calorimetry chamber

- Sample heated above critical temperature, cooled down with applied field
- Cooling rate during transition can be controlled
- Trapped flux increases residual resistance

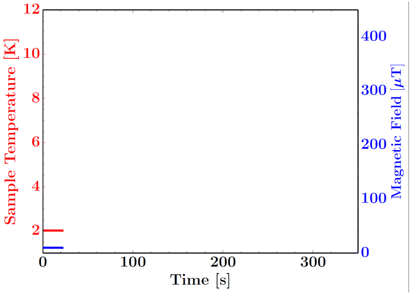

Trapped Flux Measurement

Copper solenoid and magnetometer mounted within calorimetry chamber

- Sample heated above critical temperature, cooled down with applied field
- Cooling rate during transition can be controlled
- Trapped flux increases residual resistance

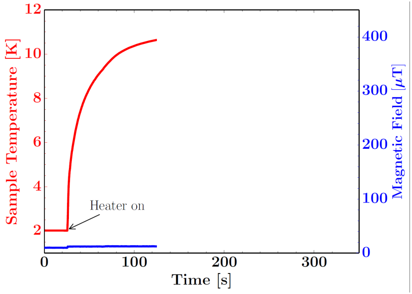

Trapped Flux Measurement

Copper solenoid and magnetometer mounted within calorimetry chamber

- Sample heated above critical temperature, cooled down with applied field
- Cooling rate during transition can be controlled
- Trapped flux increases residual resistance

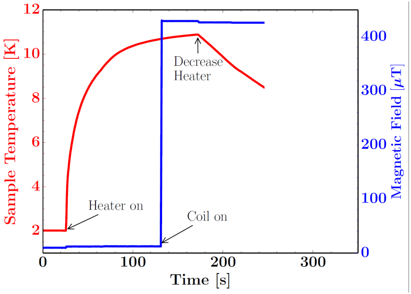

Trapped Flux Measurement

Copper solenoid and magnetometer mounted within calorimetry chamber

- Sample heated above critical temperature, cooled down with applied field
- Cooling rate during transition can be controlled
- Trapped flux increases residual resistance

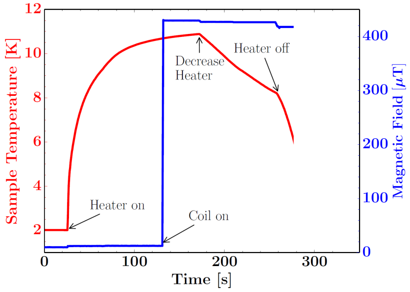

Trapped Flux Measurement

Copper solenoid and magnetometer mounted within calorimetry chamber

- Sample heated above critical temperature, cooled down with applied field
- Cooling rate during transition can be controlled
- Trapped flux increases residual resistance

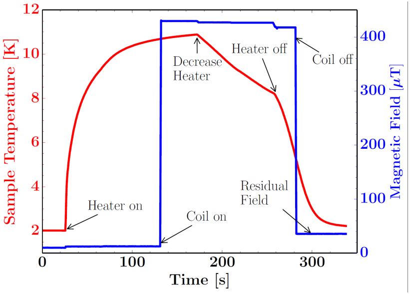

Trapped Flux Measurement

Copper solenoid and magnetometer mounted within calorimetry chamber

- Sample heated above critical temperature, cooled down with applied field
- Cooling rate during transition can be controlled
- Trapped flux increases residual resistance

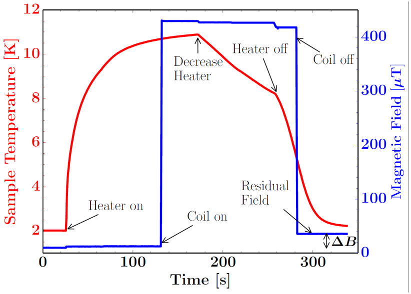

Trapped Flux Measurement

Copper solenoid and magnetometer mounted within calorimetry chamber

- Sample heated above critical temperature, cooled down with applied field
- Cooling rate during transition can be controlled
- Trapped flux increases residual resistance

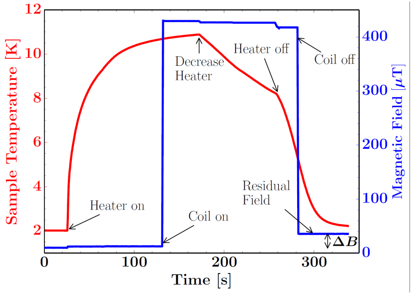

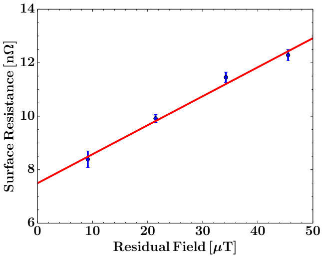

Critical Field

- RF pules with very low duty cycle and increasing field applied
- Fit data to extract $B_{C,RF}$ and T_C

$$B_C = B_C(0)\left(1 - (\frac{T}{T_C})^2\right)$$

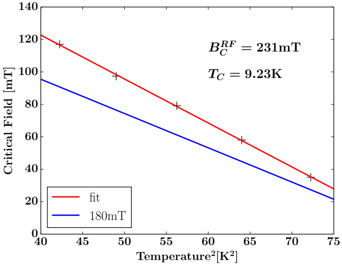

Further Measurements

Critical Field

- RF pules with very low duty cycle and increasing field applied
- Fit data to extract $B_{C,RF}$ and T_C

$$B_C = B_C(0)\left(1 - \left(\frac{T}{T_C}\right)^2\right)$$

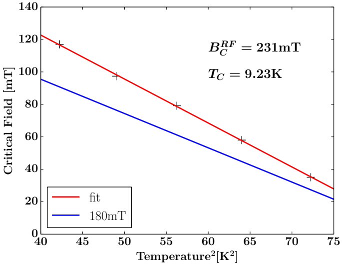

Penetration depth

- Measure resonance frequency while changing temperature of sample
- Slater Theorem and geometry factor of sample relates Δf to $\Delta\lambda_L$
- Fit with Gorter Casimir expression to obtain λ_0 and $\mathrm{T_C}$

$$\lambda_L(T) = \frac{\lambda_0}{\sqrt{1-(T/T_C)^4}}$$

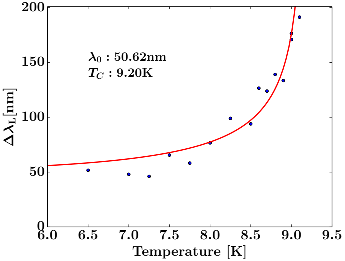

Conclusion/Outlook

QPR system at HZB commissioned:

- Field limit at 120 mT on sample surface
- Detailed characterization of large grain niobium sample

Conclusion/Outlook

QPR system at HZB commissioned:

- Field limit at 120 mT on sample surface
- Detailed characterization of large grain niobium sample

Upgrades and improvements planned:

- Add additional frequencies 850 MHz and 1300 MHz
- Ring shaped heater to minimize temperature gradient

Conclusion/Outlook

QPR system at HZB commissioned:

- Field limit at 120 mT on sample surface
- Detailed characterization of large grain niobium sample

Upgrades and improvements planned:

- Add additional frequencies 850 MHz and 1300 MHz
- Ring shaped heater to minimize temperature gradient
- New sample chambers with demountable sample

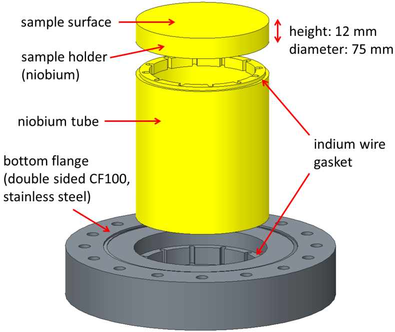

S.Keckert, TUPB067

Conclusion/Outlook

QPR system at HZB commissioned:

- Field limit at 120 mT on sample surface
- Detailed characterization of large grain niobium sample

Upgrades and improvements planned:

- Add additional frequencies 850 MHz and 1300 MHz
- Ring shaped heater to minimize temperature gradient
- New sample chambers with demountable sample

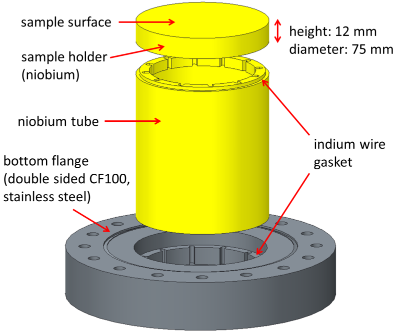

S.Keckert, TUPB067

Measurements comparing doped/undoped niobium planned

Acknowledgements

We would like to thank our colleaugues from HZB, CERN and JLab for their support towards this project

D. Pflueckhahnn, S. Rotterdam, S. Klauke

S. Aull, T. Junginger

S.Castagnola, T. Powers